Safe Mining Technology for Steeply Inclined Unstable Coal Seams

Sailei Wei[1,2]*, Lei Tan[1,2], Hai Wu[1,2], Junming Zhang[1,2]

[1] Work Safety Key Lab on Prevention and Control of Gas and Roof Disasters for Southern Goal Mines, Hunan University of Science and Technology, 411201 Xiangtan, China

[2] Department of Resources, Environment and Safety Engineering, Hunan University of Science and Technology, 411201 Xiangtan, China

* Correspondence: Sailei Wei (1622903862@qq.com)

Abstract: This study investigates the application of the horizontal stratified mining method to the extraction of steeply inclined unstable coal seams at the Puxi Mine. The stress environment in the mining area, the relationship between the supports and surrounding rock, the control of the rock layers in the caving zone, and the mechanical analysis of the roof collapse following the extraction of the steeply inclined coal seam were examined. The stress conditions in the mining area under the horizontal stratified mining method were explored, and a numerical analysis model was established using FLAC3D software, based on the rock mechanics parameters of the Puxi Mine's rock layers and strata. The results indicate that, in the stress environment of the horizontal stratified mining method, the mining area is subject to not only the self-weight stress from the surrounding strata, large horizontal ground stresses, and gas pressures, but also concentrated stresses in both the dip and strike directions. When using this mining method, the stability of the two sides of the tunnel is generally good due to the surrounding rock being of a relatively stable nature. However, the roof collapse in the upper layers during the extraction of the lower layers is one of the factors affecting the safety of the support structures in the lower layers, necessitating enhanced support management. Deformation is expected in the mining face of the lower layers during extraction, and measures must be taken to prevent any instances of roof spalling. Therefore, the horizontal stratified mining method is considered feasible for the extraction of steeply inclined unstable coal seams at the Puxi Mine.

Keywords: Steeply inclined unstable coal seams; Horizontal stratified mining method; Numerical simulation; FLAC3D

1 Introduction

Steeply inclined thin coal seams [1–3] refer to seams with an inclination greater than 45° and a thickness of less than 1.3 m [4]. Although the total reserve of steeply inclined coal seams in China is not large, they are widely distributed, especially in the southern mining regions, where 80% of mines contain such seams. The complex geological structure of these seams, combined with the inclined layering of both the coal seam and its overlying strata, creates significant challenges for mining. The heterogeneity of the rock in the horizontal direction, the stress conditions of the strata, changes in the force transmission mechanism of the overlying rock after mining, and variations in mining depth along the dip direction all contribute to the increased difficulty of extracting steeply inclined coal seams [5].

Zhao [6] introduced the primary mining methods for steeply inclined coal seams and their applicability, which included the horizontal stratified mining method [6–8]. Cui et al. [9] and Zhang [10] explored the applicability of this method for steeply inclined coal seams, achieving safe, stable, efficient, and high-quality extraction of unstable coal seams. Lai et al. [11] described the mechanical model of rock pillars and roofs during steeply inclined mining, explaining the mechanical response behaviour of key disaster-prone zones in deep working faces under the influence of deep mining dynamics. By analysing the spatial correlation of a large amount of microseismic data, the time-space response relationship controlling coal-rock dynamic failure during the advancement of the steeply inclined working face was revealed. The movement of the rock strata is highly complex during the horizontal stratified mining

of steeply inclined coal seams [12–14]. The working face can be affected by shock pressure caused by mining-induced seismic activity [15]. Cao et al. [16] conducted a case study using discrete element simulation and field investigation, studying the evolution of shock pressure from the perspectives of stress distribution, crack propagation, and coal body fragment ejection, thereby providing important references for understanding the mechanism of shock pressure-induced damage at the working face.

Taking the complex geological conditions of the Puxi Mine as an example, extensive and indepth research has been conducted on the tunnel layout of the mining area [17] and the mining technology [18]. The horizontal stratified mining method has been identified as the most suitable approach. Jia [19] explored the fundamentals and significance of rock control technology, emphasising its critical role. Therefore, a mechanical analysis of the stress conditions in the mining area was conducted in this study using FLAC3D software, with a numerical model established based on the mechanical parameters of the rock strata at the Puxi Mine. This model was used to assess the applicability and safety of applying the horizontal stratified mining method to steeply inclined and unstable coal seams [20, 21].

## 2 Mining Method for Steeply Inclined Unstable Coal Seams at Puxi Mine

The current mining methods at the mine include the strike longwall mining method and the horizontal stratified mining method. The former is the primary mining method at the mine, accounting for more than 90% of the total production, while the latter contributes only 2.1–3.73% of the total production, being applied exclusively for the extraction of steeply inclined unstable coal seams. The horizontal stratified mining method involves dividing the steeply inclined coal seam into several layers parallel to the horizontal plane. The height of each layer is controlled within a specific range, with no coal left in the roof during mining, typically around 2 m. The geological structure of the Puxi Mine is complex, with a series of synclines and anticlines forming the strike and dip directions. The coal seam exhibits a wavy pattern. The area for steeply inclined mining is small, and the coal seam is unstable and complex, preventing the formation of a conventional wall face. As a result, mining is challenging, and it is economically unfeasible. However, considering regional outburst prevention measures, Jiahe Company has decided to extract this portion of the coal seam. Based on the conditions of the coal seam, the steeply inclined coal seam is mined first. After the completion of the steeply inclined mining, the resulting horizontal stratified tunnels will be used as the return airways for the longwall mining working face.

3 Mechanical Analysis of the Horizontal Stratified Mining Method

3.1 Stress Environment in the Mining Area Using the Horizontal Stratified Mining Method

The stress environment in steeply inclined coal seams differs significantly from that in near-horizontal coal seams. Due to the influence of horizontal geological stress and geological structure, the thickness of the coal seam in steeply inclined layers varies considerably, and even the coal quality can change.

The gravity of the strata overlying the steeply inclined coal seam is a significant source of stress. As shown in Figure 1, the self-weight G of any particle in the overlying strata of the steeply inclined coal seam can be decomposed into two components: a vertical force F_1, perpendicular to the plane of the coal seam, and a force F_2, along the dip direction. As the dip angle of the coal seam increases, the force F_2 increases, while F_1 decreases. Consequently, the tunnel experiences greater lateral pressure. The displacement and collapse of the roof and floor strata generally exhibit a downward trend.

$$F_1 = G \cos \alpha \quad F_2 = G \sin \alpha$$
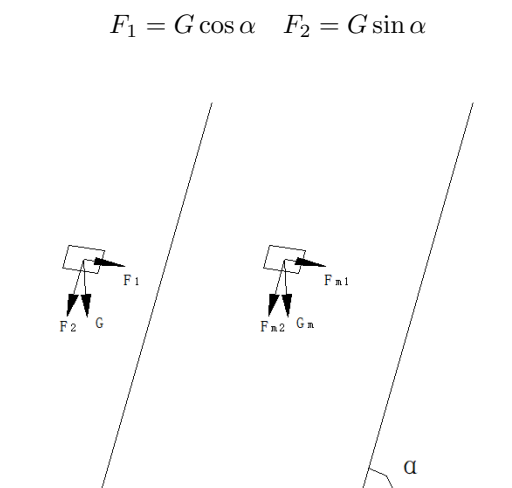
Figure 1. Gravity and its decomposed forces in the roof strata of steeply inclined coal seams

In the equation, α represents the dip angle of the coal seam.

3.2 Analysis of the Relationship Between the Support and Surrounding Rock in the Mining Area

The horizontal stratified mining method typically features a smaller length of the stratified level tunnel or mining face. The roof and floor strata of the coal seam act as the two sides of the roadway, with the overlying strata composed of collapsed loose gangue [22]. The load conditions on the support in the mining face are shown in Figure 2.

a) Calculation method for the stratified level tunnel or mining area and the mining area support load

The basic assumptions and conditions are as follows:

The gangue above the stratified level tunnel or mining area is treated as a loose medium.

Stability condition for the tunnel roof: No relative movement occurs between the gangue particles.

The dip angle of the coal seam is 90°.

b) Stress limit equilibrium theory for loose media

Under the conditions outlined above, the stress limit equilibrium theory for loose media was introduced to calculate the support load in the stratified level tunnel or mining area. The stress limit equilibrium state for loose materials refers to a state of equilibrium in which the initial shear stress and internal friction within the entire material or a specific region of it are just overcome. The appearance of this stress state causes the movement of the loose material.

At any point in the loose medium, suppose there is an arbitrary infinitesimal plane passing through this point with a normal. On this plane, normal and tangential stress components, denoted as σ_n and τ_n, act. In the case of equilibrium failure, the shear strength of the loosely bound medium along this plane follows a linear relationship.

$$|\tau_n| = \sigma_n \tan \phi + c \tag{1}$$

where, c is the cohesion of the loose medium.

If the following basic conditions are satisfied at any point in the loose medium:

$$|\tau_n| \le \sigma_n \tan \phi + c \text{ and } \sigma_n \ge -c \cot \varphi \tag{2}$$

Then the material will not undergo sliding.

For convenience, the stress limit equilibrium state of the loose medium is represented using the Mohr stress circle. The graphical method was then applied to determine the parameters that constitute the equilibrium conditions.

Figure 3 shows the Mohr stress circle. In order to simplify the problem, the envelope of all the curves was approximated by the straight line AD. From the figure, it can be observed that the shear strength line AD represents the limiting equilibrium equation.

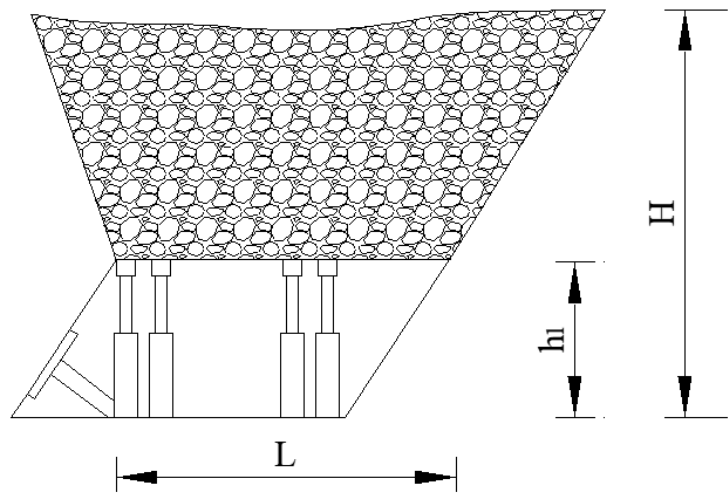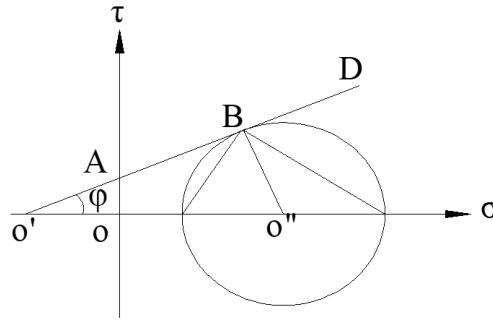$$\tau = \sigma \tan \phi + c \tag{3}$$

Figure 2. Calculation of the load on the mining face support

Figure 3. Mohr stress circle

The region above the line AD corresponds to the sliding zone, while the region below it represents the equilibrium zone. The angle of friction ϕ is the angle between the line and the horizontal axis. The initial shear strength c is represented by the line segment OA.

Further analysis of Figure 3 reveals that the sine of the maximum inclination angle can be expressed as:

$$\sin\theta_{\max} = \frac{O''B}{O'O''} \tag{4}$$

$$O''B = \frac{\sigma_1 - \sigma_3}{2} \tag{5}$$

and

$$O'O'' = O'O + OO'' = \sigma_c + \frac{\sigma_1 + \sigma_3}{2} \tag{6}$$

Thus,

$$\sin\theta_{\max} = \frac{\sigma_1 - \sigma_3}{\sigma_1 + \sigma_3 + 2\sigma_c} \tag{7}$$

From the figure, it is clear that the maximum inclination angle equals the internal friction angle ϕ. Therefore, when $\sin\theta_{\max} = \sin\phi$, another stress limit equilibrium equation can be derived:

$$\sigma_1 - \sigma_3 = (\sigma_1 + \sigma_3 + 2\sigma_c)\sin\phi \tag{8}$$

c) Lateral pressure coefficient under the stress limit state

The lateral pressure and pressure coefficient under the limit state were calculated using the relationship between the principal stresses in the loose medium's limit equilibrium state.

By substituting σ_1 and σ_3 in Eq. (3) with σ_z and σ_x and letting $\sigma_c = c\cot\phi$, the following equation can be obtained:

$$\sigma_z - \sigma_x = (\sigma_z + \sigma_x + 2c\cot\phi)\sin\phi \tag{9}$$

Solving for σ_x in this equation yields:

$$\sigma_x = \sigma_z\frac{1 - \sin\phi}{1 + \sin\phi} - 2c\frac{\cos\phi}{1 + \sin\phi} \tag{10}$$

By rewriting σ_z and the coefficient containing the internal friction angle ϕ following $2c$ in Eq. (5) and simplifying, the expression becomes:

$$\frac{1 - \sin\phi}{1 + \sin\phi} == \frac{\sin^2\left(45° - \frac{\phi}{2}\right)}{\cos^2\left(45° - \frac{\phi}{2}\right)} = \tan^2\left(45° - \frac{\phi}{2}\right) \tag{11}$$

The coefficient following $2c$ can be expressed as:

$$\frac{\cos\phi}{1 + \sin\phi} = \sqrt{\frac{1 - \sin^2\phi}{(1 + \sin\phi)^2}} = \sqrt{\frac{1 - \sin\phi}{1 + \sin\phi}} = \sqrt{\tan^2\left(45° - \frac{\phi}{2}\right)} = \tan\left(45° - \frac{\phi}{2}\right) \tag{12}$$

The substitution of Eqs. (6) and (7) into Eq. (5) results in:

$$\sigma_x = \sigma_z \tan^2\left(45° - \frac{\phi}{2}\right) - 2c\tan\left(45° - \frac{\phi}{2}\right) \tag{13}$$

$$\sigma_z = \sigma_x \tan^2\left(45° + \frac{\phi}{2}\right) + 2c\tan\left(45° + \frac{\phi}{2}\right) \tag{14}$$

For the loose medium with cohesion $c = 0$, the following expressions apply:

$$\sigma_x = \sigma_z \tan^2\left(45° - \frac{\phi}{2}\right) \tag{15}$$

$$\sigma_z = \sigma_x \tan^2\left(45° + \frac{\phi}{2}\right) \tag{16}$$

Thus, the pressure coefficient under the loose medium's limit equilibrium condition is given by:

$$K_c = \frac{\sigma_x}{\sigma_z} = \frac{1 - \sin\phi}{1 + \sin\phi} = \tan^2\left(45° - \frac{\phi}{2}\right) \tag{17}$$

d) Calculation of vertical pressure at the bottom of loose medium

In order to calculate the pressure at the bottom of a loose medium container, the Yang-Xin formula is still widely used to calculate the vertical pressure on a unit area.

$$P_z = \frac{\gamma_k S}{K_w l K_c}\left[1 - \exp\left(-\frac{K_w l K_c}{S}Z\right)\right] \tag{18}$$

where, P_z represents the vertical pressure on the unit area of the bottom plate of a container with a filling depth of Z; K_w is the friction coefficient between the bulk material and the container walls; S is the horizontal area of the bulk material; and l is the perimeter of the container's horizontal cross-section.

e) Calculation of stratified tunnel or mining area and support loads

Based on rock mechanics test parameters and combined with field experience data, the following parameter values were adopted:

For a maximum stratified tunnel or mining area height of 15 m and a maximum roof distance of 3.2 m, the calculations are as follows:

$$\phi = 25°; \quad \gamma_k = 25\text{kN/m}^3; \quad l = 10.4\text{ m}; \quad S = 6.4\text{ m}^2; \quad K_w = 0.15; \text{and } Z = 15\text{ m}$$

Therefore, the following values are obtained:

$$K_c = 0.4058, \text{and } P_z = 195\text{kN/m}^2$$

For the unit hydraulic support in the mining area and stratified tunnel, with a canopy spacing of 0.8 m, column spacing of 0.5 m, and support density of 2.5 supports per square metre, the supporting force per pillar was calculated to be 78.0 kN. This calculation indicates that the force acting on the existing single pillar is significantly below its rated value, ensuring that the strength requirements for support are met.

### 3.3 Rock layer Control in the Caving Zone

Research on rock layer control for steeply inclined coal seam mining is limited, both domestically and internationally. The study of rock layer control in the caving zone for the tunnel horizontal stratified mining of steeply inclined coal seams is, however, a novel area of research [23, 24]. The control of the caving zone rock layers is crucial to fully exploit the mining-induced pressure for breaking the roof coal, while also protecting the horizontally stratified tunnel.

When horizontal stratified mining is conducted, and the roof layer is not sufficiently filled with fallen gangue, if the coal seam roof and floor are relatively hard, the roof generally will not cave in until the fractured limit of the exposed roof layer is reached [24–26]. According to mechanical theory, the ultimate height for roof failure in the caving zone, when the roof is unsupported, is calculated as follows:

$$H_j = A \sin \beta \sqrt{\frac{[\sigma_{\mathrm{p}}]}{0.75 B \gamma \cos \beta}} \tag{19}$$

where, A is the thickness of the immediate roof's first layer (m); β is the angle of coal seam dip (degrees); B is the thickness of the immediate roof (m); σ_p is the ultimate tensile strength of the immediate roof (MPa); and γ is the bulk density of the roof rock layer (kg/m^3).

The caved gangue in the caving zone, due to the effect of its own weight, generally does not remain in place but immediately slides downward. The necessary condition for sliding to occur is $f < tga$, where f represents the dynamic friction coefficient of the fallen gangue along the coal seam floor and a is the coal seam dip angle. For mining areas, f=0.65 and a=60~900, which evidently satisfy this condition. However, the sliding of the fallen gangue does not solely depend on the dip angle, but also on the ratio of the thickness of the rock layer prior to falling, h, to the coal seam thickness, m. Studies have shown that when h/m >0.4~0.5, as shown in subgraph (a) of Figure 4, after the rock falls to the floor, it does not break into small pieces or roll but piles up or remains close to its original state. When $h/m < 0.4$ ~0.5, as shown in subgraph (b) of Figure 4, due to the large fall height, the rock fragments are more likely to break into smaller pieces, which are arranged chaotically and irregularly, and slide violently downward. This results in the filling of the lower part of the caving zone, preventing further collapse of the roof rock in that region. Meanwhile, as the free height in the upper part of the caving zone increases, the fall height may also increase (Figure 5), thereby enhancing the filling effect on the lower part [20–26].

(a)   (b)
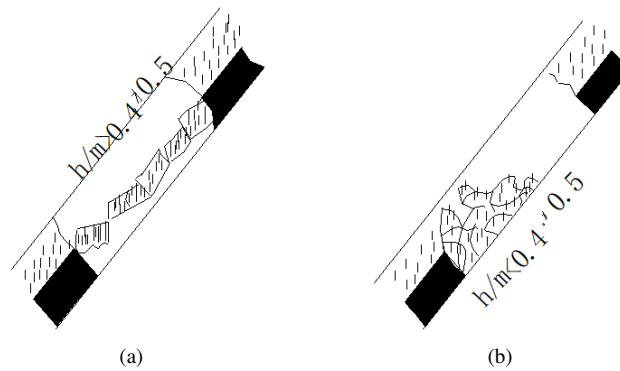
Figure 4. Movement characteristics of fallen gangue
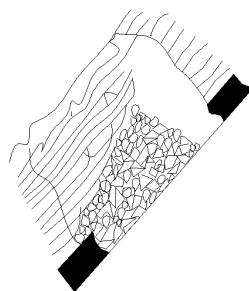
Figure 5. Impact of the sliding fallen gangue on the filling effect in the lower part of the mined-out area

3.4 Mechanical Analysis of Roof Collapse in Steeply Inclined Coal Seams

It is assumed that the shattered gangue and loose coal behave as elastic bodies, and thus, the roof can be regarded as a beam supported on an elastic foundation. Accordingly, a mechanical model of the mining area after the roof collapse was established, as shown in Figure 6.
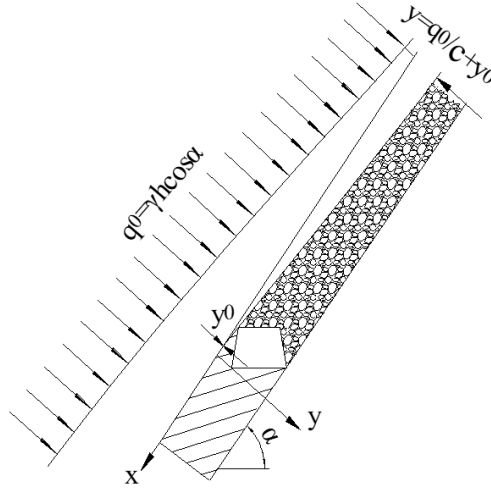

Figure 6. Mechanical model of the mining area

Based on the theory of an elastic foundation beam, for the region with $x > 0$, the differential equation of the roof deflection curve is given by:

$$EI\frac{d^4y}{dx^4} = q_0 - k_1 y \tag{20}$$

where, E and I represent the elastic modulus and the moment of inertia of the roof, respectively; q_0 is the uniform load on the roof, with $q_0 = H\gamma \cos\alpha$; and k_1 is the Winkler foundation coefficient for the real coal body.

The deflection curve equation for the roof is given by:

$$y = \frac{q_0}{k_1} + e^{-\alpha x}\left(C_1 \sin\alpha x + C_2 \cos\alpha x\right) \tag{21}$$

where, C_1 and C_1 are integration constants; and α is the resistance coefficient, with $\alpha = \sqrt[4]{k_1/4EI}$.

For the region $x < 0$, i.e., on the side of the loose roof coal, the differential equation of the roof deflection curve is:

$$EI\frac{d^4y}{dx^4} = q_0 - k_2\left(y - y_0\right) \tag{22}$$

where, k_2 is the Winkler foundation coefficient for the loose coal body; and y_0 is the roof deflection before the collapse of the top coal.

The deflection curve equation for the roof is then:

$$y = \frac{q_0}{k_2} + y_0 + e^{\beta x}\left(D_1 \sin\beta x + D_2 \cos\beta x\right) \tag{23}$$

where, D_1 and D_2 are integration constants; and β is the resistance coefficient, with $\beta = \sqrt[4]{k_2/EI}$.

When $x=0$, Eqs. (22) and (23) lead to:

$$\frac{q_0}{k_1} + C_2 = \frac{q_0}{k_2} + y_0 + D_2 \tag{24}$$

At $x=0$, the roof deflection curves on both sides smoothly connect, and the corresponding derivatives of the curves at this point are equal. This condition allows for the calculation of the integration constants.

$$\left.\begin{array}{c} \alpha\left(C_1 - C_2\right) = \beta\left(D_1 + D_2\right) \\ -\alpha^2 C_1 = \beta^2 D_1 \\ \alpha^3\left(C_1 + C_2\right) = \beta^3\left(D_1 - D_2\right) \\ y_0 = \frac{q_0}{k_1} + C_2 \\ y_0 = \frac{q_0}{k_2} + D_2 \end{array}\right\} \tag{25}$$

Solving Eq. (25) yields the following values:

$$C_1 = \frac{\beta^2(\beta - \alpha)q_0}{\alpha^2(\beta + \alpha)k_2}, \quad C_2 = \frac{\beta^2 q_0}{\alpha^2 k_2}, \quad D_1 = \frac{(\alpha - \beta)q_0}{(\alpha + \beta)k_2}, \quad D_2 = -\frac{q_0}{k_2}, \quad y_0 = \frac{q_0}{k_1} + \frac{\beta^2 q_0}{\alpha^2 k_2}$$

Substituting these integration constants into Eq. (21) and simplifying results in Eq. (26). Multiplying both sides of Eq. (26) by k gives the pressure acting on the real coal body roof:

$$y = \frac{q_0}{k_1} + \sqrt{\frac{k_2}{k_1}}\frac{q_0}{k_2}e^{-\alpha x}\left(\frac{\beta - \alpha}{\beta + \alpha}\sin\alpha x + \cos\alpha x\right) \tag{26}$$

$$p^m = ky = q_0\left[1 + \sqrt{\frac{k_1}{k_2}}e^{-\alpha x}\left(\frac{\beta - \alpha}{\beta + \alpha}\sin\alpha x + \cos\alpha x\right)\right] \tag{27}$$

From Eq. (27), it can be observed that when x=0, the maximum value of p_m occurs:

$$p^m_{\max} = q_0\left(1 + \sqrt{\frac{k_1}{k_2}}\right) \tag{28}$$

When $x \to \infty$, then $p_m = q_0$.

Substituting D_1 and D_2 into Eq. (28), both sides are multiplied by k_2 and simplified, yielding the pressure acting on the loose coal seam as:

$$p^d = q_0\left[1 - e^{\beta x}\left(\frac{\beta - \alpha}{\beta + \alpha}\sin\beta x + \cos\beta x\right)\right] \tag{29}$$

When x=0, the minimum value of p^d obtained is $p^{d0}_{\min}$.

When $x \to -\infty$, then $p^d = q_0$.

From the above analysis, it can be deduced that at x=0, the pressure acting on the loose coal body is zero, as shown in Figure 7. As the various sections of the roof collapse and the collapse process is completed, the space above the tunnel becomes filled with debris, forming a filling zone that resupports the roof and plays a role in supporting the sides of the tunnel. At this point, the tunnel is in a reduced pressure or pressure-free state.
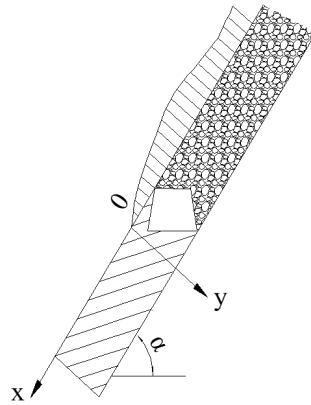
Figure 7. Pressure distribution pattern along the inclined direction after roof collapse

4 Numerical Analysis

4.1 Numerical Analysis Modelling

4.1.1 Content of the numerical analysis

The following calculations were carried out in accordance with the problems that need to be addressed in this study:

a) Stability of the surrounding rock in the mining area after the upper stratigraphic excavation and support.

b) Stability of the surrounding rock in the mining area during the lower stratigraphic excavation and support process.

4.1.2 Selection of parameters for the numerical analysis

The parameters obtained from rock mechanics experiments are the mechanical properties of the rock blocks, while the mechanical parameters required for numerical simulation are those of the rock mass. Therefore, the mechanical parameters derived from the rock mechanics experiments need to be processed. The specific values are shown in Table 1.

4.1.3 Establishment of the numerical analysis model

In order to minimise the impact of boundary constraints on the simulation results and to meet the requirements of the study, the width of the computational model was set to 50 m, with the model height adjusted according to the specific simulation needs. The model employs stress boundary conditions. A uniform vertical compressive stress was applied to the upper boundary of the model, considering the self-weight of the overlying rock mass, denoted by , where is the average volumetric force of the overlying rock layer, and is the distance from the model's upper boundary to the surface. A horizontally varying compressive stress, depending on the depth, was applied to both sides of the model. The vertical displacement at the lower boundary was fixed, while horizontal displacements were constrained on the left and right boundaries, as shown in Figure 8.

The coal seam was modelled using the Mohr-Coulomb plasticity model. The roof and floor rock layers of the coal seam were also modelled using the Mohr-Coulomb plasticity model. Excavation was modelled using the null model, with beam elements used to simulate individual props and π beams, while liner elements were used to simulate the stratified timber supports.

Table 1. Mechanical parameters of rock mass for each layer

| Rock Layer	Density $(\mathrm{kg/m^3})$	Bulk Modulus (GPa)	Shear Modulus (GPa)	Cohesion (MPa)	Friction Angle (°)	Tensile Strength (MPa)
Upper roof	2635	11.5	5.5	9.07	53	6.0
Direct roof	2210	6.2	4.2	5.74	52	3.37
Coal seam	1465	0.85	0.18	0.8	25	0.3
Direct floor	2210	6.2	4.5	5.78	52	3.37
Lower floor	2635	11.5	5.5	9.07	53	6.0
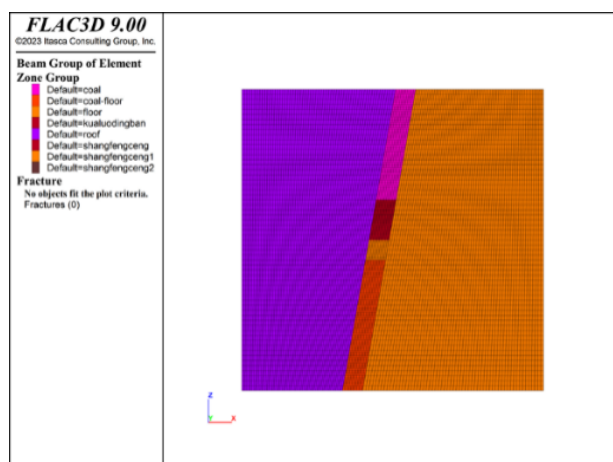
Figure 8. Numerical calculation model

4.2 Results and Evaluation of Numerical Analysis

4.2.1 Stress distribution around the mining area after upper layer mining without support

Figure 9 shows the displacement of the tunnel roof and floor, as well as the two sidewalls, after the upper layer mining under the current mining conditions. The results indicate that if the upper layer mining is not immediately supported, significant subsidence of the roof occurs, which severely affects the normal working space. Figure 9, Figure 10, Figure 11 to Figure 12 present various distributions under the condition of no support after upper layer mining, including the displacement distribution of the roof and floor, the plastic zone distribution of the roof and floor, the displacement distribution of the sidewalls, and the stress distribution of the sidewalls in the mining area.
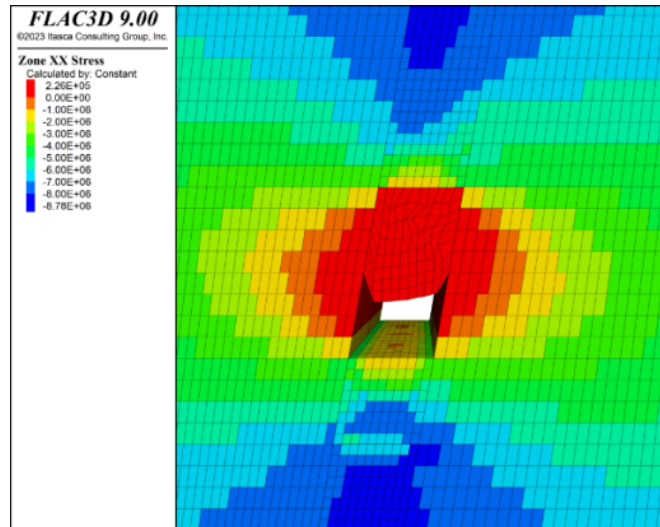
After the upper layer mining, without support, the stress environment around the working face was altered due to the removal of coal, causing a transition from a three-dimensional stress state to a two-dimensional stress state. This leads to the subsidence of the roof above the working face. Figure 10 illustrates the significant deformation of the roof, while a large plastic zone appears in the coal layer of the roof. Additionally, a certain depth of plastic zone was formed in the floor. Figure 11 and Figure 12 demonstrate that stress concentrations occur both vertically and horizontally in the surrounding rock, but due to the high strength of the sidewalls, no significant deformation is observed in these areas.
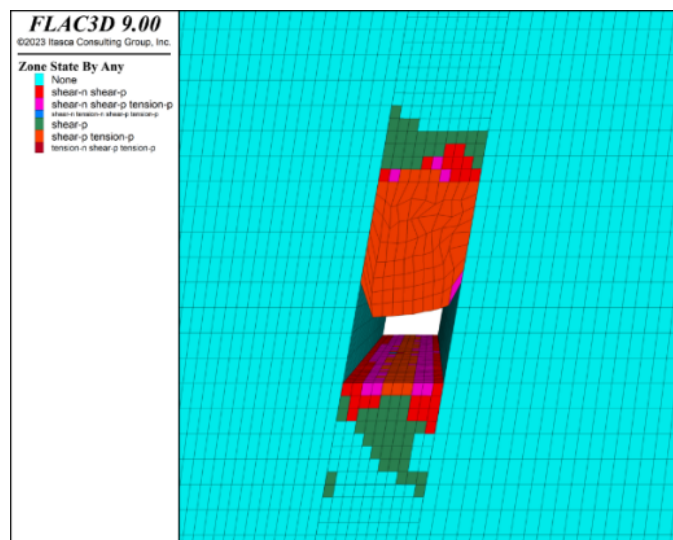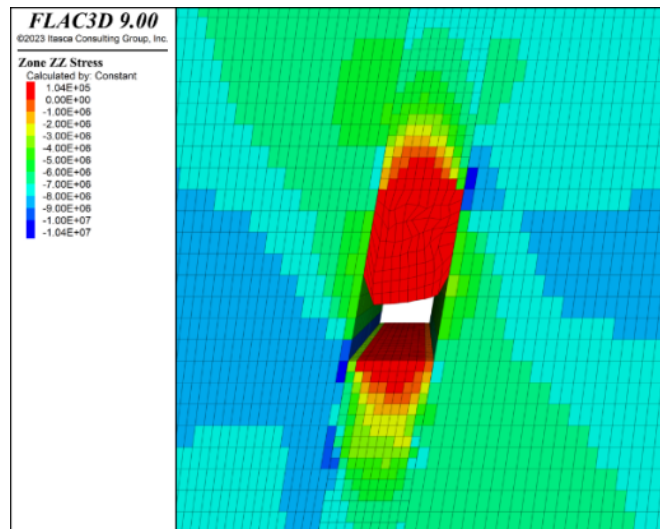

Figure 9. Distribution of the plastic zone around the mining area after upper layer mining without support
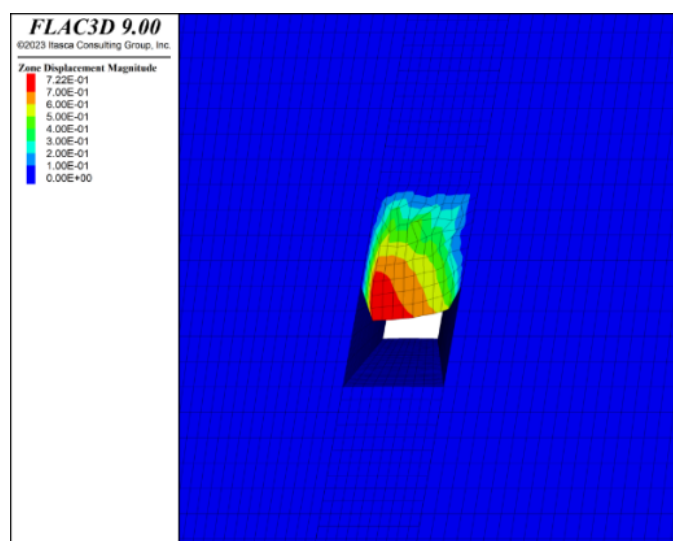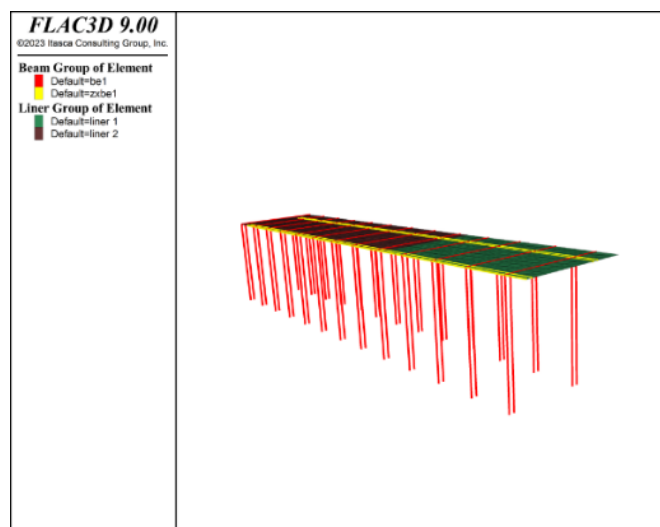

Figure 10. Displacement distribution around the mining area after upper layer mining without support

Figure 11. Distribution of horizontal stress around the mining area after upper layer mining without support

Figure 12. Distribution of vertical stress around the mining area after upper layer mining without support

Figure 13. Support structure diagram after upper layer mining with support
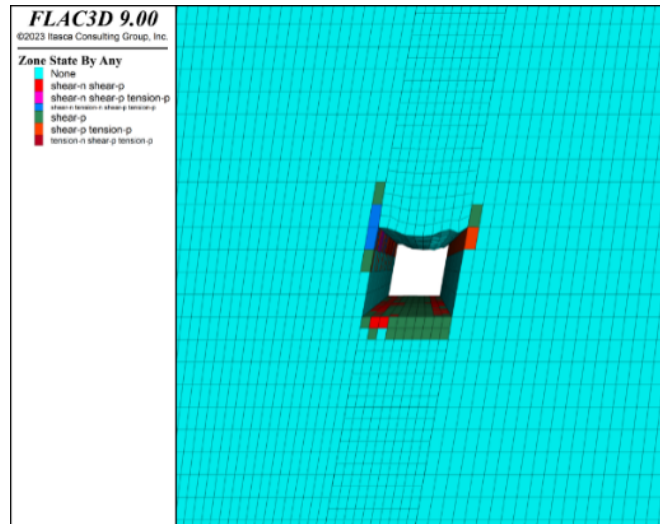
Figure 14. Distribution of plastic zones around the mining area after upper layer mining with support
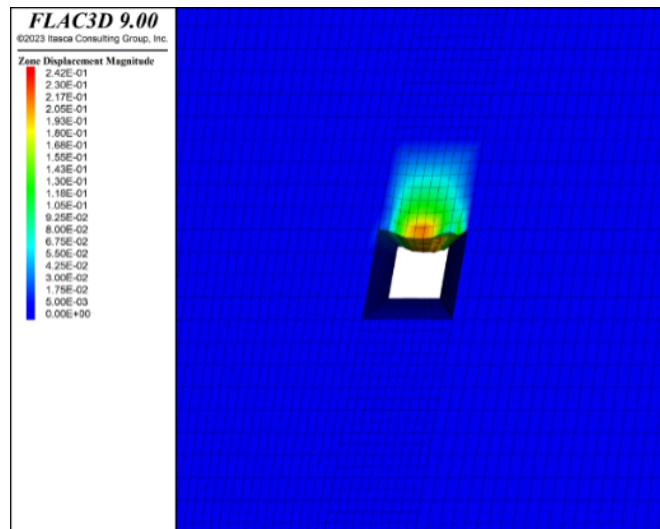

Figure 15. Distribution of displacement around the mining area after upper layer mining with support
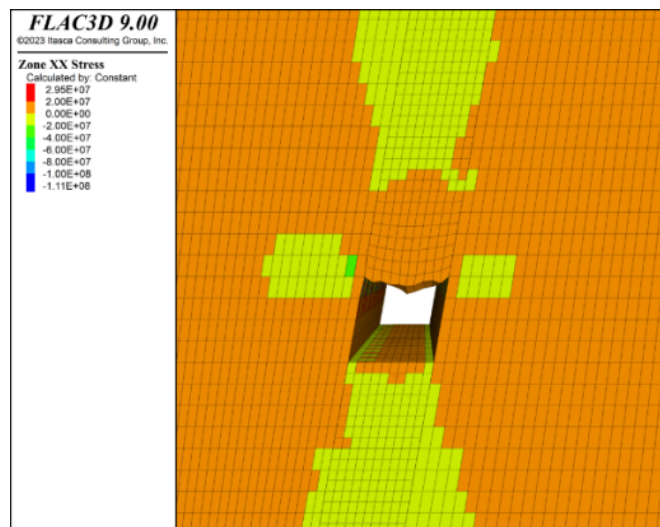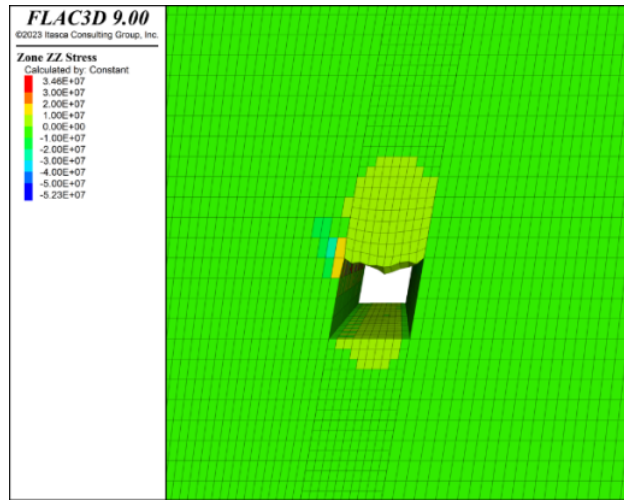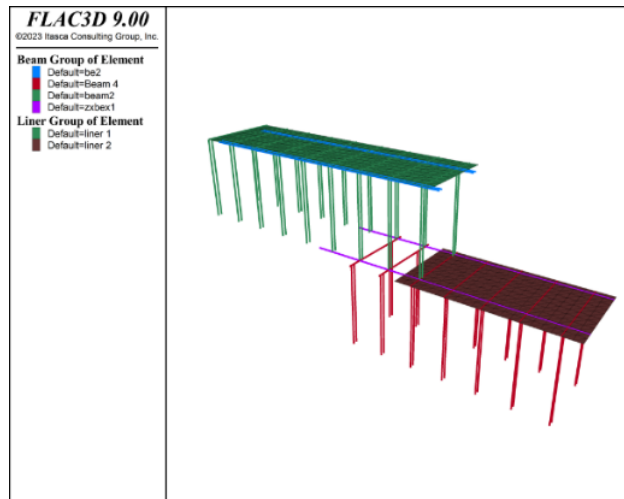

Figure 16. Distribution of horizontal stress around the mining area after upper layer mining with support

Figure 17. Distribution of vertical stress around the mining area after upper layer mining with support

Figure 18. Schematic diagram of the upper and lower layer connection after lower layer mining with support

4.2.2 Stress field distribution around the tunnel after upper layer mining with support

If timely support is implemented after upper layer mining, as shown in the support structure diagram (Figure 13), a significant reduction in the amount of roof subsidence is observed. After the application of single pillar and π beam support structures, From Figure 14, Figure 15, Figure 16 and Figure 17, the subsidence decreased substantially from 72 cm, which occurred without support, to just 5 cm. Furthermore, the plastic zone distribution on the coal roof virtually disappeared, with only a very shallow plastic zone remaining in the tunnel floor. The roof remained largely intact.

As shown in Figure 18 and Figure 19, Upon completion of the upper layer excavation, the lower layer was then mined, maintaining three rows of connected pillars between the upper and lower layers, thus forming a ventilation system with a forward and return airflow pattern. In terms of plastic zone distribution, a significant plastic zone was observed in the roof after removing the upper layer support, leading to roof collapse in this area. The collapsed roof material accumulated on the support structures in the lower layer, forming an artificial false roof, which ensures the stability of the lower layer support system. Additionally, a relatively deep plastic zone was also observed in the unmined coal body of the lower layer, which facilitates the subsequent mining of the lower layer.

Upon commencement of lower layer excavation, Figure 20 and Figure 21 demonstrate the presence of stress reduction zones around the mining area in both the upper and lower layers. This phenomenon facilitates the support process, as only a relatively small supporting resistance is required to maintain the stability of the mining area.

The displacement distribution around the mining area after lower layer mining indicates significant displacement in the roof after the removal of support in the upper layer. Additionally, at the step between the upper and lower layers, substantial axial deformation of the coal body occurs. This necessitates careful attention to the stability of the lower layer excavation face during mining to prevent sidewall collapse incidents.
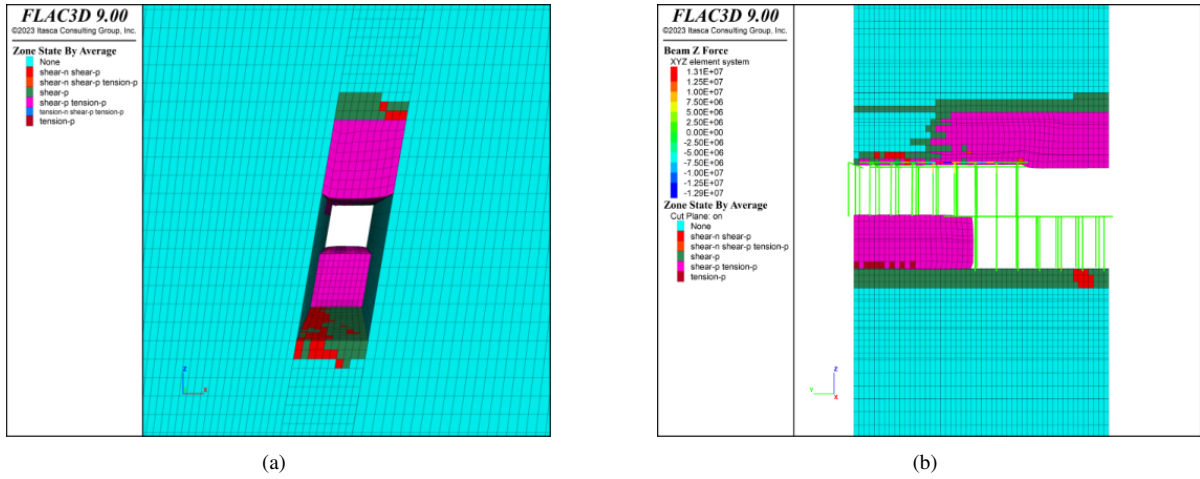
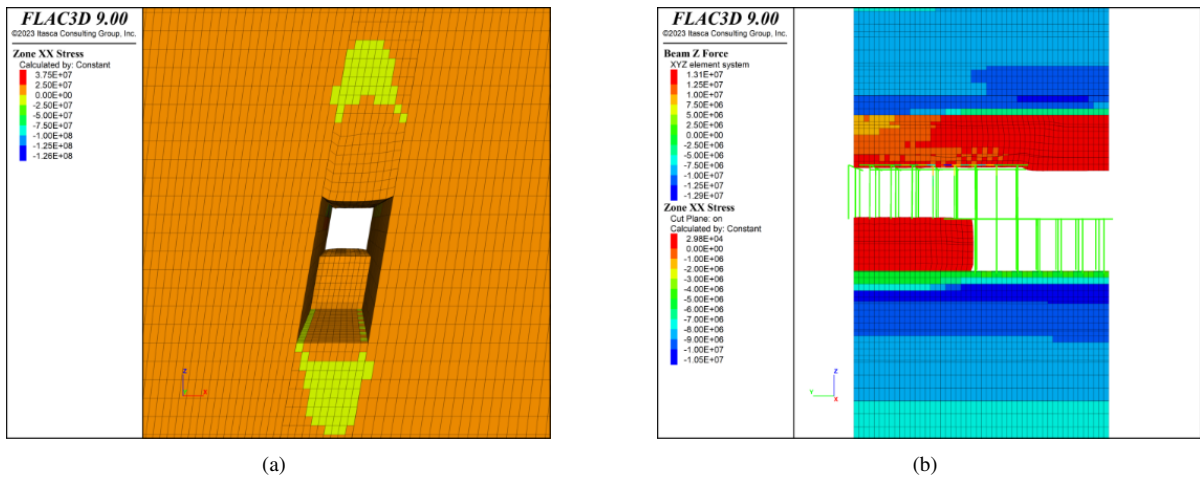**Figure 19.** Distribution of plastic zones around the mining area after lower layer mining with support

Figure 20. Distribution of horizontal stress around the mining area after lower layer mining with support
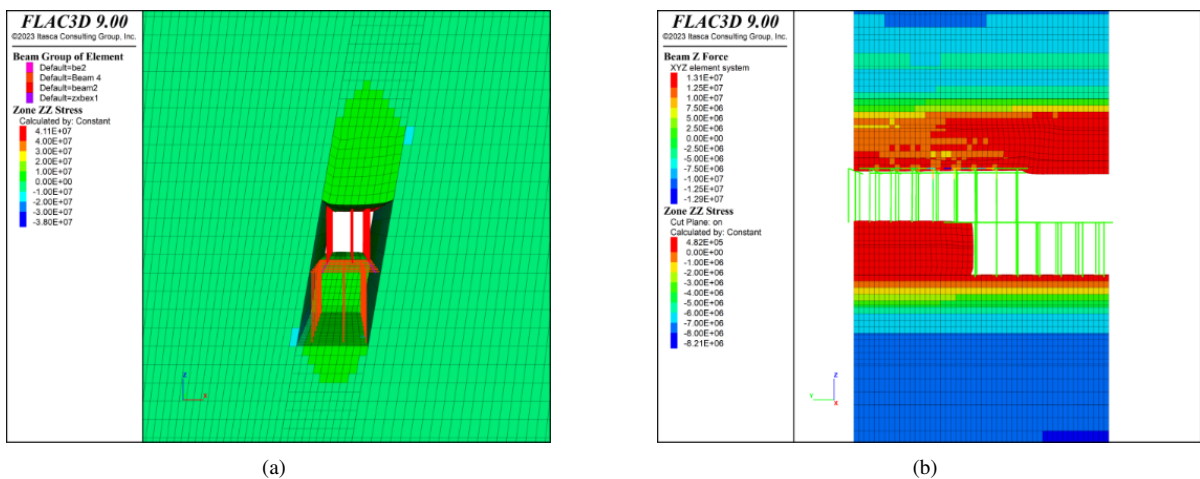

Figure 21. Distribution of vertical stress around the mining area after lower layer mining with support

A "top-down" problem exists at the junction of the upper and lower layers' support structures. As shown in Figure 22 and Figure 23, the support beams are located between the roof and floor of the coal seam. During mining, the stress in the roof and floor decreases due to coal excavation, thus maintaining relative stability. Consequently,

the support beams remain stable due to the two fixed sections. In the direction of the face advance, the crossbeam is partly located on the floor of the upper layer and partly on the roof of the lower layer, forming a cantilever beam structure. Therefore, collapse is prevented in the direction of face advance. Despite the high height of the support structure at the junction of the upper and lower layers, it remains in a stable state.
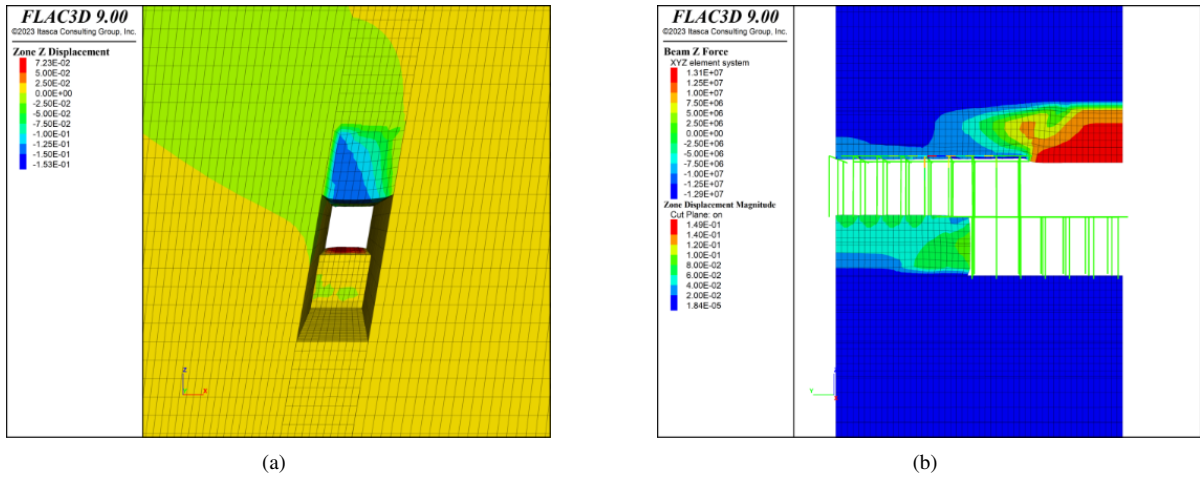

(a)

(b)

Figure 22. Distribution of displacement around the mining area after lower layer mining with support
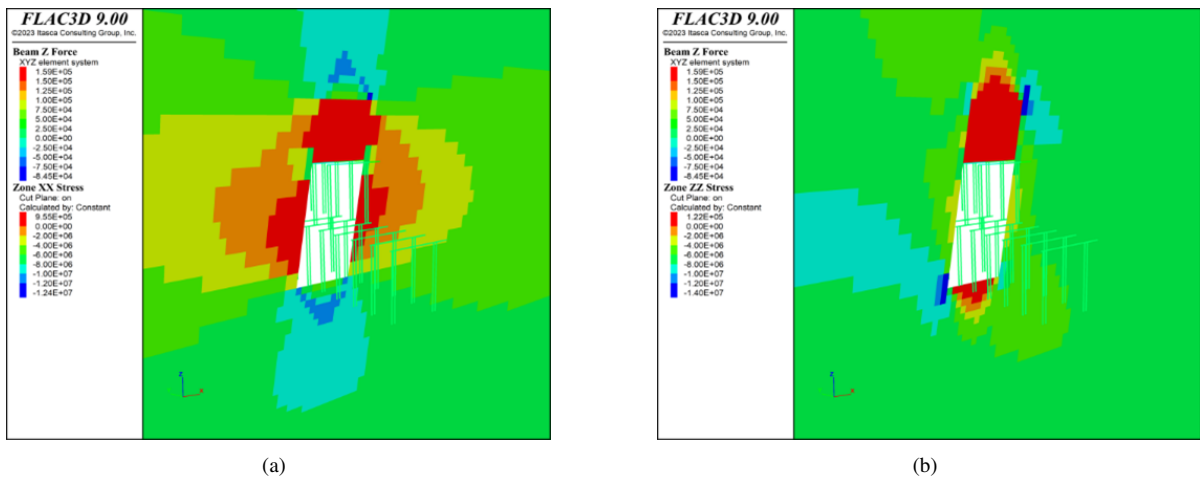

(a)

(b)

Figure 23. Distribution of XX and ZZ stress at the junction of the upper and lower layers after lower

5 Conclusion

In the stress environment of the mining area using the horizontal stratified mining method, in addition to bearing the self-weight stress, significant horizontal ground stress, and gas pressure from the overlying strata, concentrated stress is also experienced along the inclined and strike directions of the mining area. The most significant manifestation of mining-induced pressure occurs during the prop-drawing caving process. The dynamic pressure acts on the lower-layer horizontal tunnels. However, field production practice shows that the impact of dynamic pressure on the tunnels is relatively weak. Therefore, the rational determination of tunnel support structures is crucial to maintaining the stability of the horizontal stratified tunnels, reducing maintenance costs, and improving mining efficiency.

When mining is conducted using this method, the stability of the tunnels is generally good as the two sides of the mining area are composed of rock. During the extraction of the lower layer, the collapse of the roof in the upper layer becomes a significant factor affecting the safety of the lower-layer support structure, necessitating enhanced on-site support management. The mining face of the lower layer experiences some deformation, and measures must be taken to prevent sidewall collapse. Thus, the use of the horizontal stratified mining method at the Puxi mine for the extraction of its steeply inclined unstable coal seams is deemed feasible.

Data Availability

The data used to support the research findings are available from the corresponding author upon request.

Conflicts of Interest

The authors declare no conflict of interest.

References

[1] H. Wu, Q. Jia, W. Wang, N. Zhang, and Y. Zhao, "Experimental test on nonuniform deformation in the tilted strata of a deep coal mine," *Sustainability*, vol. 13, no. 23, p. 13280, 2021. https://doi.org/10.3390/su132313280

[2] H. Wu, X. Wang, W. Yu, W. Wang, Z. Zhang, and G. Peng, "Analysis of influence law of burial depth on surrounding rock deformation of road-way," *Adv. Civ. Eng.*, vol. 2020, no. 1, p. 8870800, 2020. https://doi.org/10.1155/2020/8870800

[3] B. P. Xu, "Research and application of mining method for sharp tilted thin coal seam," *Value Eng.*, vol. 38, no. 17, pp. 161–163, 2019. https://doi.org/10.14018/j.cnki.cn13-1085/n.2019.17.040

[4] D. Kong, Y. Xiong, Z. Cheng *et al.*, "Stability analysis of coal face based on coal face-support-roof system in steeply inclined coal seam," *Geomech. Eng.*, vol. 25, p. 233, 2021. https://doi.org/10.12989/GAE.2021.25.3.233

[5] X. H. Chi and X. Meng, "Development trend of steeply inclined thin coal seam mining methods," *Shanxi Archit.*, vol. 42, no. 12, pp. 48–50, 2016. https://doi.org/10.13719/j.cnki.cn14-1279/tu.2016.12.027

[6] B. Zhao, "Logic analysis of mining pressure manifestation in gently inclined thin coal seam fully mechanized mining face," *Energy Energy Conserv.*, no. 3, pp. 69–72, 2023. https://doi.org/10.16643/j.cnki.14-1360/td.2023.03.052

[7] H. Yan, G. C. Li, Y. Q. Li, O. C. Zhang, and C. Q. Zhu, "Stress evolution characteristics of the intensively mining-induced surrounding roadways within an extra-thick coal seam: A case study from the Tashan coal mine, China," *J. Cent. South Univ.*, vol. 30, no. 11, pp. 3840–3854, 2023. https://doi.org/10.1007/s11771-023-5472-8

[8] W. Yan, J. Chen, Y. Tan, W. Zhang, and L. Cai, "Theoretical analysis of mining induced overburden subsidence boundary with the horizontal coal seam mining," *Adv. Civ. Eng.*, vol. 2021, no. 3, pp. 1–7, 2021. https://doi.org/10.1155/2021/6657738

[9] F. Cui, X. P. Wang, J. Cao, and P. Shan, "Analysis of the disturbance impact of horizontal segmented fully mechanized top coal mining in steeply inclined coal seams," *J. Min. Saf. Eng.*, vol. 32, no. 4, pp. 610–616, 2015. https://doi.org/10.13545/j.cnki.jmse.2015.04.014

[10] H. Zhang, "Research on the application of water splitting coal mining method in unstable coalbeds," *Shandong Coal Sci. Technol.*, no. 5, p. 2, 2015. https://doi.org/10.3969/j.issn.1005-2801.2015.05.24

[11] X. Lai, H. Xu, P. Shan, Q. Hu, W. Ding, S. Yang, and Z. Yan, "Research on the mechanism of rockburst induced by mined coal-rock linkage of sharply inclined coal seams," *Int. J. Miner. Metall. Mater.*, vol. 31, no. 5, pp. 929–942, 2024. https://doi.org/10.1007/s12613-024-2833-8

[12] W. H. Yang, X. P. Lai, J. T. Cao, H. C. Xu, and X. W. Fang, "Study on evolution characteristics of overburden caving and void during multi-horizontal sectional mining in steeply inclined coal seams," *Thermal Sci.*, vol. 24, no. 6 Part B, pp. 3915–3921, 2020. https://doi.org/10.2298/TSCI2006915Y

[13] Y. Hu, G. Wang, J. Chen, Z. Liu, C. Fan, and Q. Cheng, "Prediction of gas emission from floor coalbed of steeply inclined and extremely thick coal seams mined using the horizontal sublevel top-coal caving method," *Energy Sources Part A Recovery Utilization and Environ. Effects*, 2020. https://doi.org/10.1080/15567036.2020.1733143

[14] Z. Wang, L. Dou, and G. Wang, "Coal burst induced by horizontal section mining of a steeply inclined, extra-thick coal seam and its prevention: A case study from Yaojie No. 3 coal mine, China," *Shock Vib.*, vol. 2019, no. PT.2, pp. 1–13, 2019. https://doi.org/10.1155/2019/8469019

[15] K. Z. Song, F. X. Li, L. M. Zhu, and M. S. Wang, "Analysis of the sensitivity of influencing factors on tunnel secondary lining structure stress," *J. Highway Transp. Res. Dev.*, vol. 8, no. 4, pp. 69–75, 2014. https://doi.org/10.1061/JHTRCQ.0000413

[16] J. Cao, L. Dou, G. Zhu, J. He, S. Wang, and K. Zhou, "Mechanisms of rock burst in horizontal section mining of a steeply inclined extra-thick coal seam and prevention technology," *Energies*, vol. 13, no. 22, p. 6043, 2020. https://doi.org/10.3390/en13226043

[17] S. Yan, J. Bai, X. Wang, and L. Huo, "An innovative approach for gateroad layout in highly gassy longwall top coal caving," *Int. J. Rock Mech. Min. Sci.*, vol. 59, pp. 33–41, 2013. https://doi.org/10.1016/j.ijrmms.2012.11.007

[18] Z. Wei, K. Yang, X. Chi, W. Liu, and X. Zhao, "Dip angle effect on the main roof first fracture and instability in a fully-mechanized workface of steeply dipping coal seams," *Shock Vib.*, 2021. https://doi.org/10.1155/2021/5557107

[19] Y. Jia, "Surrounding rock control technology of strong dynamic pressure roadway in Hudi coal industry," *World J. Eng. Technol.*, vol. 12, no. 2, pp. 362–372, 2024. https://doi.org/10.4236/wjet.2024.122023

[20] X. Li, C. Wang, C. Li, C. Yong, Y. Luo, and S. Jiang, "Mining technology evaluation for steep coal seams based on a GA-BP neural network," *ACS Omega*, vol. 9, no. 23, pp. 25 309–25 321, 2024. https://doi.org/10.1021/acsomega.4c03167

[21] Z. Zhang, Y. Liu, W. Y. Zhu, J. Liu, and C. X. Xie, "Experimental study of prevention and control of rock burst in steeply inclined coal seams by mining sequence and filling," *Shock Vib.*, 2022. https://doi.org/10.1155/2022/2450513

[22] S. H. Luo, Y. P. Wu, K. Z. Liu, X. P. S., and L. Ding, "Study on the shape of the space stress arch shell in steeply dipping coal seam mining," *J. China Coal Soc.*, vol. 41, no. 12, 2016. https://doi.org/10.13225/j.cnki.jccs.2016.0539

[23] L. H. Kong, F. X. Jiang, S. H. Yang, J. W. Song, and C. W. Wang, "Movement of roof strata in extra-thick coal seams in top-coal caving mining based on a high precision micro-seismic monitoring system," *J. Univ. Sci. Technol. Beijing*, vol. 32, no. 5, pp. 552–558, 588, 2010. https://doi.org/10.13374/j.issn1001-053x.2010.05.014

[24] S. Yang, N. Xu, H. Liu, X. Zhang, and S. Mei, "Research and application of 'three zones' range within overlying strata in goaf of steep coal seam," *Front. Energy Res.*, vol. 12, 2024. https://doi.org/10.3389/fenrg.2024.1333016

[25] W. Lv, K. Guo, Y. Wu, Y. Tan, K. Ding, and B. Li, "Compression characteristics of local filling gangue in Steeply Dipping Coal Seam," *Energy Explor. Exploit.*, vol. 40, no. 4, pp. 1131–1150, 2022. https://doi.org/10.1177/01445987211073627

[26] H. Wang, Y. Wu, J. Jiao, and P. Cao, "Stability mechanism and control technology for fully mechanized caving mining of steeply in-clined extra-thick seams with variable angles," *Min. Metall. Explor.*, vol. 38, pp. 1047–1057, 2020. https://doi.org/10.1007/s42461-020-00360-0